Formation energy and optical excitation mechanisms of Er in GaN semi-bulk crystals

Y. Q. Yan, J. Li, J. Y. Lin, et al.

View Online

Export Citation

CrossMark

QBLOX

1 qubit

Shorten Setup Time
Auto-Calibration
More Qubits

Fully-integrated
Quantum Control Stacks
Ultrastable DC to 18.5 GHz
Synchronized <<1 ns
Ultralow noise

100s qubits

visit our website >

AIP
Publishing

Formation energy and optical excitation mechanisms of Er in GaN semi-bulk crystals

Y. Q. Yan, (iD) J. Li, (iD) J. Y. Lin, (iD) and H. X. Jiang[a) (iD)

AFFILIATIONS

Department of Electrical and Computer Engineering, Texas Tech University, Lubbock, Texas 79409, USA

[a)]Author to whom correspondence should be addressed: hx.jiang@ttu.edu

ABSTRACT

Erbium (Er) doped GaN (Er:GaN) bulk crystals are promising as an optical gain material for high energy lasers. Other than the preferred configuration of Er^{3+} occupying the Ga site with four nearest neighbor N atoms (Er_{Ga}), Er can also form a complex with a defect (Er_{Ga}-DX) in Er:GaN. A set of Er:GaN semi-bulk crystals were grown by hydride vapor phase epitaxy (HVPE) at different growth temperatures to allow the determination of the formation energies, E_F, of Er optical centers in Er:GaN. Photoluminescence (PL) emission spectra near 1.5 μm pumped by a near band edge excitation ($\lambda_{exc} = 375$ nm) and by a resonant excitation ($\lambda_{exc} = 980$ nm) were measured, which yielded two different formation energies of $E_F = 2.8$ eV and 3.3 eV, corresponding to the formation of Er_{Ga}-DX and Er_{Ga} in Er:GaN, respectively. As a gain medium, the formation of Er_{Ga}-DX in Er:GaN would not only reduce the pumping efficiency of Er optical centers but also increase the optical loss. Our results provide useful insights into possible strategies for enhancing the fraction of Er_{Ga} in Er:GaN and, hence, the pumping efficiency, paving the way for achieving optical gain and lasing in Er:GaN.

Published under an exclusive license by AIP Publishing. https://doi.org/10.1063/5.0077742

Doped in a solid host, the intra 4f shell transitions from the first excited state ($^4I_{13/2}$) to the ground state ($^4I_{15/2}$) of Er^{3+} ions emit light in the 1.5 μm region, which lies in the spectral range of minimum transmission loss in silica-based optical fibers.[1–3] Accordingly, Er doped materials have been extensively investigated for applications in optical communication devices, including optical amplifiers and emitters active in the 1.5 μm spectral region.[1–3] It has been demonstrated that the emission intensities associated with the Er intra 4f shell transitions in Er doped GaN (Er:GaN) have a negligible thermal quenching[4–7] due to the outstanding mechanical and thermal properties of the GaN host.[8] Additionally, 1.54 μm wavelength is considered relatively "eye-safe," as the upper limit of eye-safe laser exposure at 1.5 μm is more than 4 orders of magnitude higher than that of the wavelengths ranging below or close to 1 μm.[9,10] As such, Er:GaN semi-bulk crystals have been studied recently as a gain medium for high energy lasers and illuminators operating in the 1.5 μm spectral region with expected applications encompassing communications, security, defense, manufacturing, and health/medicine.[11–13]

To obtain emission from the Er intra 4f shell transitions near 1.5 μm, optically active Er^{3+} in Er:GaN can be excited by two different excitation schemes: (1) a non-resonant pump via a band-to-band (or band edge) excitation of the semiconductor host through a non-radiative energy transfer of free carriers (or excitons) to nearby Er^{3+} and (2) a resonant pump via a direct excitation of electrons from a lower lying Stark energy level to a higher level among $^4I_{11/2}$, $^4I_{13/2}$, and $^4I_{15/5}$ states within the 4f manifold of Er^{3+}. For instance, in Er doped YAG crystals, 980 nm laser sources are widely utilized to achieve optical lasing near 1.5 μm because the 980 nm photon energy matches the energy difference between the ground state ($^4I_{15/2}$) and the second excited state ($^4I_{11/2}$) and, hence, can provide a direct excitation of electrons from ($^4I_{15/2}$) to ($^4I_{11/2}$) state within the Er inner 4f shell. Previous theoretical and experimental studies have indicated that not only an Er atom can substitute onto the Ga sublattice with four nearest neighbor N atoms to form an isolated optical center of Er_{Ga}, but Er can also form a defect complex center involving a nitrogen vacancy or dislocation, Er_{Ga}-DX.[14,15] It was further shown that the emission at 1.54 μm from the isolated Er_{Ga} optical center can be excited by either mechanism, whereas the emission at 1.54 μm from the defect-related Er optical center, Er_{Ga}-DX, can only be observed through a band-to-band or band edge excitation.[16] The present study focuses on studying the differences between these two pumping mechanisms, including the formation energies, energy transfer processes, advantages, and disadvantages, which have not been extensively explored.

Er:GaN semi-bulk wafers of 2-in. in diameter with a thickness of 10 μm were grown by hydride vapor phase epitaxy (HVPE) along the [0001] direction of GaN with a growth rate of ~15 μm/h. Prior to the

deposition of Er:GaN, a GaN epilayer of 3 μm in thickness was first grown on sapphire substrate by metal-organic chemical vapor deposition (MOCVD). For the HVPE growth of the Er:GaN layer, the Er and Ga metals react with HCl gas and the reactants were carried by hydrogen gas to the growth zone. The growth temperatures were varied from 1060 to 1180 °C for a set of seven Er:GaN samples, while other growth conditions remain the same. The Er doping concentrations [Er] of selective samples were profiled by secondary ion mass spectroscopy (SIMS) measurements performed by Evans Analytical Group.

Room temperature PL emission spectra around 1.5 μm region were first measured under a non-resonant (near band edge) excitation using a laser diode operating at $\lambda_{exc} = 375$ nm. The PL emission was collected using an InGaAs detector in conjunction with a spectrometer proving a spectral resolution of 3 nm. In this excitation scheme, free carriers and free excitons are first generated in the GaN host followed by the energy transfer to the nearby Er^{3+} via non-radiative processes. Figure 1(a) plots the PL spectra in the 1.5 μm region for three representative Er:GaN samples grown at different growth temperatures of $T_g = 1060$ °C (red), 1100 °C (blue), and 1160 °C (black). The results revealed that the Er emission at 1.5 μm increases with an increase in T_g. To unveil the detailed growth temperature effect, we present in Fig. 1(b) the Arrhenius plot of the PL peak emission intensity at 1.54 μm, I_{emi}, for a set of 7 Er:GaN samples grown at different temperatures of $T_g = 1060$, 1080, 1100, 1120, 1140, 1160, and 1180 °C. The

results clearly showed that the emission intensity at 1.54 μm as a function of the growth temperature, T_g, can be well described by a thermal activation behavior as follows:

$$I_{emi} = N \times e^{-E_F/kT_g}, \quad (1)$$

where k is the Boltzmann constant and N is a constant, which is linked with all possible sites available for Er atoms in GaN during growth. In Eq. (1), we define E_F as the formation energy of Er optical sites in Er:GaN. The fitting between the experimental data and Eq. (1) yielded a value of the formation energy of $E_F \sim 2.8$ eV for a non-resonant excitation at $\lambda_{exc} = 375$ nm.

To investigate the Er emission under a resonant excitation, we measured the PL emission spectra for the same set of Er:GaN samples under excitation using a laser diode operating at $\lambda_{exc} = 980$ nm, which provides a direct excitation of electrons from the ground state ($^4I_{15/2}$) to the second excited state ($^4I_{11/2}$) within the 4f manifold of Er^{3+} without invoking a non-radiative energy transfer in the GaN host. The PL spectra of Er:GaN samples grown under three representative growth temperatures, $T_g = 1060$ (red), 1100 (blue), and 1160 (black), are plotted in Fig. 2(a). Similar to the results shown in Fig. 1, the Er emission intensity at 1.5 μm increases with an increase in T_g. The Arrhenius plot of the PL peak emission intensity at 1.54 μm for the same set of 7 Er:GaN samples under 980 nm excitation is shown in Fig. 2(b), which reveals that the emission intensity increases more rapidly with T_g than for the 375 nm excitation shown in Fig. 1(b). The obtained data can be

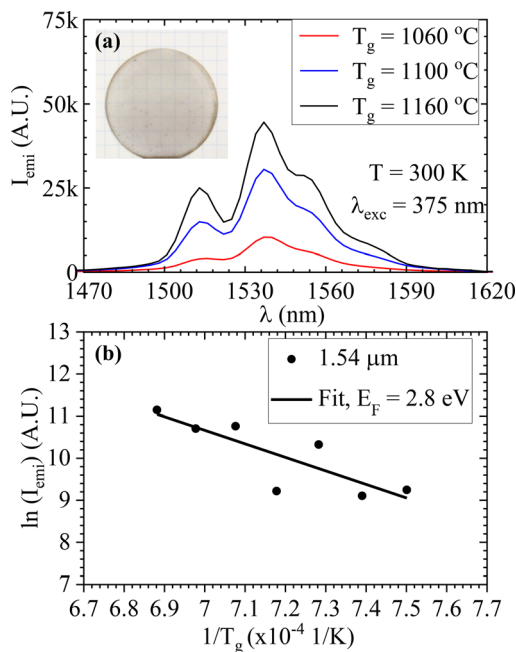**FIG. 1.** (a) PL emission spectra of three representative Er:GaN samples grown at 1060 (red), 1100 (blue), and 1160 °C (black) measured in the wavelength range of 1470 to 1620 nm excited by a laser diode operating at $\lambda_{exc} = 375$ nm. (b) The Arrhenius plot of PL emission intensities at 1.54 μm for seven Er:GaN samples grown at temperatures of 1060, 1080, 1100, 1120, 1140, 1160, and 1180 °C ($\lambda_{exc} = 375$ nm). The measured values are displayed in solid circles, and the solid line is the least squares fit of data with Eq. (1). The inset in (a) is an optical image of an as-grown Er:GaN wafer of 2-in. in diameter produced by HVPE.
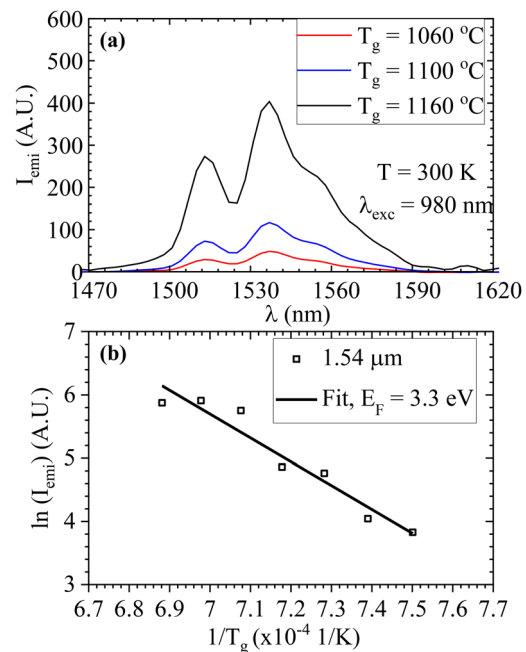

FIG. 2. (a) PL emission spectra of Er:GaN samples measured in the wavelength range of 1470 to 1620 nm for three representative samples grown at 1060 (red), 1100 (blue), and 1160 °C (black) excited by a laser diode operating at $\lambda_{exc} = 980$ nm. (b) The Arrhenius plot of PL emission intensities at 1.54 μm for seven Er:GaN samples grown at temperature of 1060, 1080, 1100, 1120, 1140, 1160, and 1180 °C ($\lambda_{exc} = 375$ nm). The measured values are displayed in open squares, and the solid line is the least squares fit of data with Eq. (1).

fitted well with Eq. (1), from which a fitted value of the formation energy $E_F \sim 3.3$ eV has been obtained.

The emission intensity at 1.5 μm must be directly proportional to the optically active Er^{3+} concentration in Er:GaN. The results shown in Figs. 1 and 2, therefore, suggest that the optically active Er^{3+} concentration in Er:GaN increases exponentially with the increase in T_g following the relationship described by Eq. (1). On the other hand, the concentration of Er^{3+} active optical centers is expected to be directly proportional to the Er doping concentration in Er:GaN. To verify this point, we plot in Fig. 3 the PL emission intensity at 1.5 μm, I_{emi}, for the samples with available SIMS data as a function of the Er concentration [Er] for both the non-resonant and resonant excitation schemes. The results shown in Fig. 3 clearly revealed that the emission intensity at 1.5 μm increases linearly with the Er concentration in Er:GaN for both excitation schemes. Therefore, to the first order, the measured E_F value should be comparable to the thermal activation energy of Er vapor pressure, which is about 3 eV.[5,6] The E_F values deduced from Figs. 1 and 2 (of 2.8 and 3.3 eV, respectively) are indeed quite close to 3.0 eV.

We believe that the observation of two different formation energies under non-resonant and resonant excitation schemes is due to the presence of two different types Er optical sites in Er:GaN samples grown by HVPE, namely, the isolated (Er_{Ga}) and defect-related (Er_{Ga}-DX) optical centers. Since the emission at 1.54 μm from the defect-related Er optical center, Er_{Ga}-DX, can only be observed

through a band-to-band or band edge excitation,[16] the observed $E_F \sim 2.8$ eV under the band edge excitation can, therefore, be attributed predominantly to the formation energy of Er-defect complexes in Er:GaN. On the other hand, since 980 nm photons provide a direct excitation of electrons from the ground state [$^4I_{15/2}$] to the second excited state [$^4I_{13/2}$] within the Er inner 4f shell, the observed formation energy of 3.3 eV under 980 nm excitation is predominantly determined by the formation of the isolated optical centers of Er_{Ga} in Er:GaN.

The observed lower formation energy of the Er-defect complexes than that of the isolated Er_{Ga} in GaN seems to be consistent with a previous study, which revealed that Er^{3+} ions tend to accumulate around threading dislocations and defects,[15] inferring that the presence of threading dislocations, defects, and strain promotes the formation and, hence, lowers the formation energy of the Er-defect complexes. Moreover, under a near band edge excitation at $\lambda_{exc} = 375$ nm, the excitation photons possess a large optical absorption coefficient in GaN of about $\alpha \sim 10^4$/cm[17] and, hence, a small optical absorption length ($l = 1/\alpha$) of ~ 1 μm. In such a scenario, only Er ions inside this thickness region are being excited, which is expected to contain more surface defects than the interior of the sample.

In contrast, the optical absorption coefficient of 980 nm resonant excitation photons in Er:GaN samples is the product of the Er concentration [Er] and excitation cross section of $\sigma_{exc} = 2.2 \times 10^{-21}$ cm^2 at 980 nm.[18] For instance, the optical absorption coefficient for 980 nm photons is $\alpha = 0.44$ cm^{-1} for an Er doping concentration of 2×10^{20} cm^3, which provides an optical absorption length ($l = 1/\alpha$) of about 2.3 cm. Therefore, the typical absorption length (or photon penetration depth) of 980 nm photons in Er:GaN is many orders of magnitude larger than a value of ~ 1 μm for photons with $\lambda_{exc} = 375$ nm. As such, all Er_{Ga} optical centers inside the Er:GaN samples can be excited by 980 nm photons and consequently the surface effects become negligible for a resonant excitation. In a more extremely case, the 1.54 μm PL emission intensity under an above bandgap excitation ($\lambda = 263$ nm) has been monitored previously in very thin Er:GaN epilayers of 0.5 μm in thickness grown at different growth temperatures by MOCVD, which revealed a value of about 1.8 eV for the formation energy for the Er-defect complex optical centers in thin GaN epilayers.[19] The results, thus, suggest that the formation energy of the optically active Er^{3+} centers in Er doped III-nitrides not only depends on the thermal activation energy of the Er vapor pressure but also depends on the type of optical centers as well as the environments in the GaN crystal host. It is important to note that these two types of optical centers in Er:GaN cannot be distinguished by SIMS measurements since SIMS can only probe the total Er concentration and is unable to distinguish different Er optical sites.

Table I compares parameters and differences between the non-resonant and resonant excitation schemes. To utilize Er:GaN as a lasing medium, since the output optical power and density are directly correlated with the volume of the optical gain medium and, hence, the absorption length of the excitation photons, the comparison results shown in Table I signifies that a higher optical power can be achieved by using a resonant excitation scheme (e.g., $\lambda_{exc} = 980$ nm), whereas the band edge excitation will be limiting the usable thickness of the Er:GaN crystal to only a few micrometers. Therefore, a resonant excitation is the desired optical pumping mechanism for Er:GaN to achieve high energy lasers.
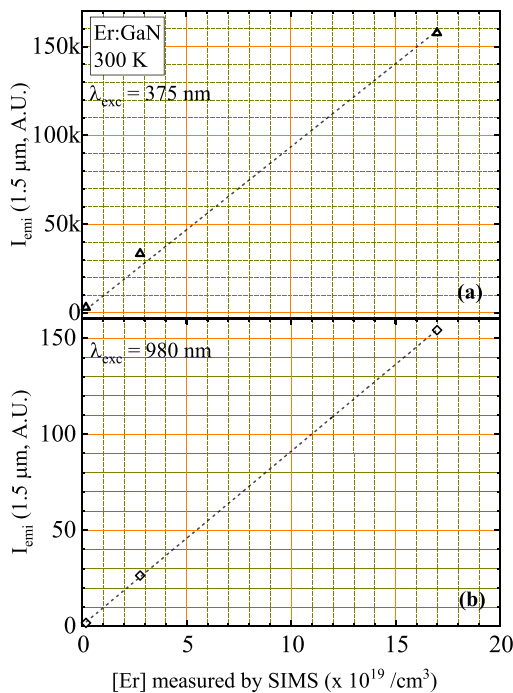

FIG. 3. (a) PL emission intensity at 1.54 μm vs Er concentration, I_{emi} vs [Er], under a non-resonant (near band edge) excitation at $\lambda_{exc} = 375$ nm. (b) PL emission intensity at 1.54 μm vs Er concentration, I_{emi} vs [Er], under a resonant excitation at $\lambda_{exc} = 980$ nm. Dashed lines are linear fittings, indicating that the PL emission intensity at 1.54 μm, I_{emi}, is linearly proportional to the Er concentration [Er] for both non-resonant and resonant excitation schemes.

TABLE I. Comparisons of parameters, properties, and mechanisms under resonant excitation ($\lambda_{exc} = 980$ nm) vs near band edge excitation ($\lambda_{exc} = 375$ nm) for Er:GaN semi-bulk crystals, where Er^{3+*}, Er_{Ga}, and V_N denote, respectively, an excited state of Er^{3+} ions, and Er^{3+} occupying the Ga site, and nitrogen vacancies in Er:GaN.

properties λ_{exc}	980 nm	375 nm
Excitation mechanism	$Er^{3+} \rightarrow Er^{3+*}$	e–h pair or exciton $\rightarrow Er^{3+*}$
Absorption length	>1 cm	$\sim 1\,\mu m$
Formation energy, E_F	3.3 eV	2.8 eV
Er configuration	Er_{Ga}	Er_{Ga} + defect (e.g., $Er_{Ga} - V_N$)
Heat generation	Low	High
Power output	High	Low
Power density	High	Low
Depth	Bulk	Surface
Surface effect	Low	High

Many other factors should also be considered, such as heat generation under optical pumping, which can be described in terms of the quantum defect (QD). QD is defined as $QD = 1 - \lambda_{pump}/\lambda_{laser}$, where λ_{pump} and λ_{laser} are pumping and lasing emission wavelengths, respectively. For a lasing line near 1.54 μm, QD for a near band edge pump at $\lambda_{pump} = 375$ nm is 75.6%, while QD (= 36.3%) is much lower for the resonant pump at $\lambda_{pump} = 980$ nm. Thus, heat generation for $\lambda_{exc} = 980$ nm is much lower than that of $\lambda_{exc} = 375$ nm. Moreover, a near band edge excitation can also excite other impurities in GaN and is strongly influenced by the surface effect because it takes place only near the sample surface. These together could further reduce the pumping efficiency and increase the optical loss.

The presence of defects and dislocations not only facilitates the formation of the less desired Er-DX optical centers in Er:GaN but also increases the optical loss in Er:GaN gain medium. Understanding the different formation energies and excitation mechanisms of Er optical centers in GaN provides useful insights into crystal growth strategies to further optimize the material quality of Er:GaN crystals for high energy laser applications. Based on our findings, the PL emission at 1.54 μm increases more rapidly with an increase in the growth temperature for the resonant excitation at $\lambda_{exc} = 980$ nm than for the near band edge excitation at $\lambda_{exc} = 375$ nm. Therefore, increasing the growth temperature is expected to enhance the ratio of Er_{Ga} to Er_{Ga}-DX and, hence, the overall performance of Er:GaN as an optical gain medium for high energy lasers operating at 1.5 μm.

In summary, the formation energies of Er optical centers in GaN have been probed by the PL emission spectroscopy for a set of seven Er:GaN samples grown under different growth temperatures. It was found that the resonant ($\lambda_{exc} = 980$ nm) excitation and near band edge ($\lambda_{exc} = 375$ nm) excitation result in two different formation energies of $E_F = 3.3$ eV and $E_F = 2.8$ eV, respectively. These two different formation energies correspond to two different Er configurations in Er:GaN, one being the isolated optical center Er_{Ga} (Er atom occupying Ga site with four nearest neighbor N atoms) and the other being the Er-defect complex. Excitation and emission mechanisms associated

with these two different Er optical centers were investigated and analyzed. The results revealed that a resonant excitation scheme (e.g., $\lambda_{exc} = 980$ nm) is preferred for Er:GaN gain medium, as it is capable of providing a much larger optical penetration depth to enable the utilization of all Er optical centers in the gain medium, lower quantum defect and, hence, lower heat generation, reduced surface and impurity effects and reduced optical loss, and, therefore, higher output optical power and power density.

AUTHOR DECLARATIONS
Conflict of Interest

We have no conflicts of interest to disclose.

DATA AVAILABILITY

The data that support the findings of this study are available within this article.

REFERENCES

[1]E. Desurvire, *Erbium-Doped Fibre Amplifiers: Principles and Applications* (John Wiley & Sons, 1994).

[2]R. J. Mears, L. Reekie, I. M. Jauncey, and D. N. Payne, Electron. Lett. **23**, 1026 (1987).

[3]P. C. Becker, N. A. Olsson, and J. R. Simpson, *Erbium-Doped Fibre Amplifiers: Fundamentals and Technology* (Academic Press, 1999).

[4]P. N. Favennec, H. L'Haridon, M. Salvi, D. Moutonnet, and Y. L. Guillou, Electron. Lett. **25**, 718 (1989).

[5]J. D. MacKenzie, C. R. Abernathy, S. J. Pearton, U. Hommerich, X. Wu, R. N. Schwartz, R. G. Wilson, and J. M. Zavada, Appl. Phys. Lett. **69**, 2083 (1996).

[6]A. J. Steckl, J. C. Heikenfeld, D. S. Lee, M. J. Garter, C. C. Baker, Y. Q. Wang, and R. Jones, IEEE J. Sel. Top. Quantum. Electron. **8**, 749 (2002).

[7]C. Ugolini, N. Nepal, J. Y. Lin, H. X. Jiang, and J. M. Zavada, Appl. Phys. Lett. **89**, 151903 (2006).

[8]H. Shibata, Y. Waseda, H. Ohta, K. Kiyomi, K. Shimoyama, K. Fujito, H. Nagaoka, Y. Kagamitani, R. Simura, and T. Fukuda, Mater. Trans. **48**, 2782 (2007).

[9]Y. Kalisky and O. Kalisky, Opt. Eng. **49**, 091003 (2010).

[10]J. A. Zuclich, D. J. Lund, and B. E. Stuck, Health Phys. **92**, 15 (2007).

[11]Z. Y. Sun, J. Li, W. P. Zhao, J. Y. Lin, and H. X. Jiang, Appl. Phys. Lett. **109**, 052101 (2016).

[12]Z. Y. Sun, Y. Q. Yan, W. P. Zhao, J. Li, J. Y. Lin, and H. X. Jiang, Appl. Phys. Lett. **112**, 202103 (2018).

[13]Y. Q. Yan, T. B. Smith, J. Li, J. Y. Lin, and H. X. Jiang, AIP Adv. **10**, 125006 (2020).

[14]J. S. Filhol, R. Jones, M. J. Shaw, and P. R. Briddon, Appl. Phys. Lett. **84**, 2841 (2004).

[15]B. Mitchell, D. Timmerman, W. Zhu, J. Y. Lin, H. X. Jiang, J. Poplawsky, R. Ishii, Y. Kawakami, V. Dierolf, J. Tatebayashi, S. Ichikawa, and Y. Fujiwara, J. Appl. Phys. **127**, 013102 (2020).

[16]D. K. George, M. D. Hawkins, M. McLaren, H. X. Jiang, J. Y. Lin, J. M. Zavada, and N. Q. Vinh, Appl. Phys. Lett. **107**, 171105 (2015).

[17]J. F. Muth, J. H. Lee, I. K. Shmagin, R. M. Kolbas, H. C. Casey, Jr., B. P. Keller, U. K. Mashra, and S. P. DenBaars, Appl. Phys. Lett. **71**, 2572 (1997).

[18]R. Hui, R. Xie, I. W. Feng, Z. Y. Sun, J. Y. Lin, and H. X. Jiang, Appl. Phys. Lett. **105**, 051106 (2014).

[19]C. Ugolini, I. W. Feng, A. Sedhain, J. Y. Lin, H. X. Jiang, and J. M. Zavada, Appl. Phys. Lett. **101**, 051114 (2012).